AD-A148 295 LOW COST GYROCOMPASS(U) GYROART INC AGOURA CA 1/1
J F KISHEL JUN 84 GYR-001 ETL-0355 DAAK70-83-C-0168

UNCLASSIFIED F/G 17/7 NL

END
DATE
FILMED
1-85
DTIC

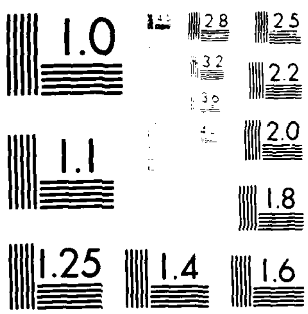

MICROCOPY RESOLUTION TEST CHART

ETL-0355

AD-A148 295

Low cost gyrocompass

E T L

Gyroart Inc.
27 Oakleaf Avenue
Agoura, California 91301

June 1984

Prepared for

U.S. ARMY CORPS OF ENGINEERS
ENGINEER TOPOGRAPHIC LABORATORIES
FORT BELVOIR, VIRGINIA 22060-5546

U.S. ARMY ENGINEER TOPOGRAPHIC LABORATORIES
ETL

84

UNCLASSIFIED

SECURITY CLASSIFICATION OF THIS PAGE (When Data Entered)

REPORT DOCUMENTATION PAGE		READ INSTRUCTIONS BEFORE COMPLETING FORM
1. REPORT NUMBER ETL-0355	2. GOVT ACCESSION NO. AD-A148 295	3. RECIPIENT'S CATALOG NUMBER
4. TITLE (and Subtitle) LOW COST GYROCOMPASS		5. TYPE OF REPORT & PERIOD COVERED Final Report Oct 1983 - May 1984
		6. PERFORMING ORG. REPORT NUMBER GYR 001
7. AUTHOR(s) Joseph F. Kishel		8. CONTRACT OR GRANT NUMBER(s) DAAK70-83-C-0168
9. PERFORMING ORGANIZATION NAME AND ADDRESS Gyroart Inc. 27 Oakleaf Ave. Agoura, CA 91301		10. PROGRAM ELEMENT, PROJECT, TASK AREA & WORK UNIT NUMBERS
11. CONTROLLING OFFICE NAME AND ADDRESS U.S. Army Engineer Topographic Laboratories Fort Belvoir, VA 22060-5546		12. REPORT DATE June 1984
		13. NUMBER OF PAGES 35
14. MONITORING AGENCY NAME & ADDRESS(if different from Controlling Office)		15. SECURITY CLASS. (of this report) Unclassified
		15a. DECLASSIFICATION DOWNGRADING SCHEDULE

16. DISTRIBUTION STATEMENT (of this Report)

Approved for public release; distribution is unlimited.

17. DISTRIBUTION STATEMENT (of the abstract entered in Block 20, if different from Report)

18. SUPPLEMENTARY NOTES

19. KEY WORDS (Continue on reverse side if necessary and identify by block number)

Azimuth
Gyrocompass
Gyroscope
North-finding

20. ABSTRACT (Continue on reverse side if necessary and identify by block number)

This report summarizes study and analysis efforts that were directed towards using gyrotechnology to define true north to an accuracy of 2 milliradians in two minutes' time in the presence of vibration environments encountered on launch vehicles. It concludes that a device could be fabricated to meet stated requirements by using a design approach that avoids the dynamics problems inherent in all pendulous suspensions for the gyro.

DD FORM 1 JAN 73 1473 EDITION OF 1 NOV 65 IS OBSOLETE

UNCLASSIFIED

SECURITY CLASSIFICATION OF THIS PAGE (When Data Entered)

TABLE OF CONTENTS

APPENDICES

APPENDIX A

Design of Flexure Suspension

APPENDIX B

Servo Designs

APPENDIX C

Gyro Drift Stability Test Data

APPENDIX D

Kalman Filter Design

APPENDIX E

Experimental Evaluation of the Static Efficiency of the Gyroart Rectilinear-Flexure Suspension

A-1

PREFACE

This study was conducted under contract DAAK70-83-C-0168 "Low Cost Gyrocompass."

The study was done during the period October 1983 - May 1984 under the supervision of Mr. Fred Gloeckler and Mr. Ray Godfrey of the US Army Engineer Topographic Laboratories, Fort Belvoir, Virginia.

LOW COST GYROCOMPASS

INTRODUCTION

This study of a low cost gyrocompass was initiated in FY 83 as an exploratory development effort. The objective was to develop a design concept and associated error budget for a portable low cost gyrocompass that would tolerate significant base motions such as those present on a modern battlefield. Studies and tests were performed to evaluate the features of the design concept. This report is a summary of that effort, including findings on gyrocompass performance capabilities under operational environments.

BACKGROUND

Portable gyrocompasses presently in the Army inventory do not meet many of the required characteristics concerning precision measurement of azimuth in the presence of base motion (vibration), base tilt, and base tilt rates. The proposed system appears to have the required capability.

INVESTIGATION

CLIN 001 of the contract required that a study and report be made on the performance of a gyrocompass under a set of operating conditions defined in general in section C of the contract as follows: The first three standard conditions called for operation (a) at any latitude between the arctic and antarctic circles ($\pm 67^\circ$ latitude), (b) in climates listed in AR-70-38, (c) after handling and transportation. The new requirement called for operation on a tripod or as part of a weapon system subject to vibration and other motions imparted by engine idling, wind, personnel movement, etc. Representative operationsl environments include

(1) Low frequency (.1 Hz.) wind motion (trailer) .0015" peak to peak.

(2) Wind induced motion at trailer resonance (4.5 to 6 Hz.) .008" peak to peak.

(3) Engine idling.

(4) Off level tilt up to $\pm 10^\circ$.

(5) Tilt rates 1.2 miliradians per minute about any horizontal axis.

(6) Ability to maintain azimuth reference when rotated or moved after gyrocompassing.

Additional requirements related to portability included

Size - 350 cubic inches.

Weight - 6 pounds.

Power - 24 V DC, 15 watts.

These portability requirements are well within the state-of-the-art at this time.

DESIGN CONCEPT

The basic approach takes advantage of the principle employed in the design of vibration-measuring equipment such as the seismograph used to record earthquakes. The natural frequency of the spring-mass-damper assembly contained within the device is made at least a factor of ten less than the frequency of the vibrations to be measured. In that case the mass suspended on the spring does not move with repect to inertial space and therefore movement of the base with respect to the mass could be recorded by a stylus attached to the mass writing on a graph paper on the frame of the instrument. The important feature applicable to a gyrocompass is that the suspended mass (gyroscope) is not disturbed by vibratory motion of the base.

Early Approach

The initial design approach employed an inverted pendulum to support the gyro. The low natural frequency required was achieved by balancing the gravity torque acting on the inverted pendulum mass against the stiffness of a flexure suspension at the base of the pendulum. Dynamic analysis revealed that while the gyro did not share the translatory motions of the base, the gyro did however rotate about its input axis because of rotations imparted to the pendulum by the vibratory inputs at the flexure suspension. At .008" double amplitude and 6 Hz. the angular rates into the gyro were intolerably high. That approach was therefore without merit.

New Design Concept - (Rectilinear Flexure)

In the new design concept the gyro is now mounted on a flexure supported platform that forms the upper horizontal arm of a parallelogram. Spring loaded flexures are the vertical arms of the parallelogram. The result is that the gyro can only translate under vibratory inputs and therefore the gyro remains parallel to the base. The rotations present in the early design concept are entirely absent. The required low natural frequency is due to the large compliance of the flexures. The same number of parts is involved in both the early and new designs. Only a trivial rearrangement is required to obtain this desirable result. The proprietory details are given in appendix A of this report.

ADDITIONAL INVESTIGATIONS

While the prime focus of the study was the design of the gyro suspension system, additional investigations were directed at other basic features of a practical gyrocompass. The results of these efforts are summarized in the appendices. These include preliminary designs for three servo systems, gyro drift stability analysis, analysis of gyrocompassing in the presence of tilt, and Kalman filter design.

PERFORMANCE UNDER OPERATIONAL ENVIRONMENTS

(1) Low frequency (.1 Hz.) wind-induced motion (trailer) .0015" peak to peak. The new rectilinear flexure suspension and gyro mass will have a natural frequency of about .01 Hz. due to the relatively high compliance of the spring loaded flexure. Thus the translational input to the gyro will be about .5% of the .0015" displacement. However, the corresponding angular displacement of the rectilinear flexure and gyro will be negligible (less than 10^{-8} radians). The corresponding angular rates are less than $.001^{\circ}$/hr.

(2) Wind-induced motion at trailer resonance (4.5 to 6 Hz.) .008" peak to peak. Again the rectilinear flexure comes to the aid of this design. The gyro translates less than .1% of the .008" displacement. The corresponding angular displacement of the rectilinear flexure and gyro due to tolerances is again negligible (less than 10^{-6} radians). The corresponding angular rate is less than .012 /hr.

(3) Vibration inputs due to engine idling. The frequency of the linear disturbance is several orders of magnitude greater than the rectilinear flexure suspension and gyro mass assembly. Thus the gyro moves (translates) a very small (less than .01% of the disturbance) amount. The corresponding angular displacement of the flexure due to imperfections in the mechanism (tolerances) is less than 10^{-8} radians. The corresponding angular rate could approach .06°/hr. This is well within the capability of the Kalman filter to suppress down to .006°/hr. or less.

(4) Off level tilt (up to 10°). The forcer and flexure systems are capable of measuring case tilt angles in this range (±10°) to an accuracy of 10^{-4} radians (20 arc seconds). The corresponding north seeking error is

$$10^{-4} \tan\lambda = 2.36 * 10^{-4} \text{ radians or .2 milliradians}$$

(5) Tilt rates 1.2 milliradians per minute. By measuring the slope of the tilt angle versus time curve by least squares procedures, the tilt rate is established. An accuracy of .05% of rate has been shown by analysis. This corresponds to .0025°/hr. or .25 mils north seeking error.

(6) Ability to maintain azimuth reference when rotated or moved after gyrocompassing. The gyroart mechanization utilizes a two degree of freedom dry tuned gyro. This permits use of one axis as the "east" or north seeking axis while the other axis is used in an azimuth stabilization loop for maintaining azimuth reference when the system is moved or rotated in azimuth.

ERROR BUDGET FOR GYRCART I

One Sigma Values - Latitude = 45°

Source	Tolerance	North Error (milliradians)
Gyro Bias (short term)	.002 °/hr.	.2
Tilt Measurement Error	20 Arc Seconds (at 10° tilt)	.1
Azimuth Synchro Readout Error	3 Minutes of Arc	.8
Tilt Rate Error	.05% of 1.5 $\frac{mil}{min}$	.25
Linear Vibration Induced Rates (6 Hz. at .008")	.012 °/hr.	1.2 mils
Angular Vibration Induced Rates (1 °/sec)	.0036 °/hr.	.36

RSS 1.52 mils

CONCLUSIONS

Accuracy of a simple north-finding gyrocompass that is based on a pendulous gyro suspension is severly degraded by external linear vibrations. Any displacement of the point of support of the pendulum results in angular rotations of the suspended gyro. For typical vibratory inputs to be found in a battlefield environment the induced angular rates can only be suppressed by long averaging times that are not compatable with tactical applications.

The current design concept for the Gyroart I employs a parallelogram-type suspension for the gyro. Thus, vibratory inputs produce only small translational inputs to the gyro without any rotation of the suspended gyro. This is a significant breakthrough in simple gyrocompass design for battlefield use. External angular vibration inputs to the gyro are also heavily attenuated by a crossed-spring flexure on the east-west axis of the gyro. Gyroart I will perform to an accuracy of two mils in two minutes time under expected battlefield environments.

APPENDIX A

Design of Flexure Suspension

I. Brief Description of Gyroart Mechanism

Figure A-1 depicts one recent version of the Gyroart mechanism. The design has evolved in several stages through a continuing process of refinement. The gyro (Kearfott Conex) is mounted on rectilinear flexures via a pair of rotary flexures. Isoelastic springs provide the compressive loads on the rectilinear flexures. Tension loads are applied to the rotary flexures.

Tilt of the main housing is measured by a centering servo system that consists of a pair of LVDT's amplifiers and electromagnetic forcers. The current through the forcers provide a measure of tilt angle since it measures the force required to hold the gyro assembly centered in the inner housing.

The Conex gyro provides an azimuth torque signal to provide azimuth stabilization of the inner housing. The Conex gyro also provides an east-west sensing axis that is used to perform the north-finding function. An electronic capture loop around the gyro east axis provides the required signals. Thus, there are three servo loops; tilt, azimuth stabilization, and east axis capture loop. Preliminary designs for these servo loops are given in appendix B.

II. Analysis of a New Rectilinear Suspension for the Gyro

Earlier study indicated that the pendulous gyro suspension does not isolate the gyro from external lateral disturbances. While the gyro mass does not translate under the vibration inputs, the pendulum forces the gyro to rotate at rates too high to be absorbed by the Kalman filter. However, by making a simple change to the basic gyro suspension system, the gyro mounting surface is now made to execute pure translations rather than rotations because of lateral vibration inputs. This eliminates the angular rate inputs to the gyro almost completely. The figures on the following page show both horizontal and vertical cross-sections through pairs of flexures to illustrate both the problem generated by the pendulous suspension and the elegant solution provided by the new rectilinear-parallelogram suspension.

BILL OF MATERIAL		
ITEM NO.	NO. REQ'D	DESCRIPTION

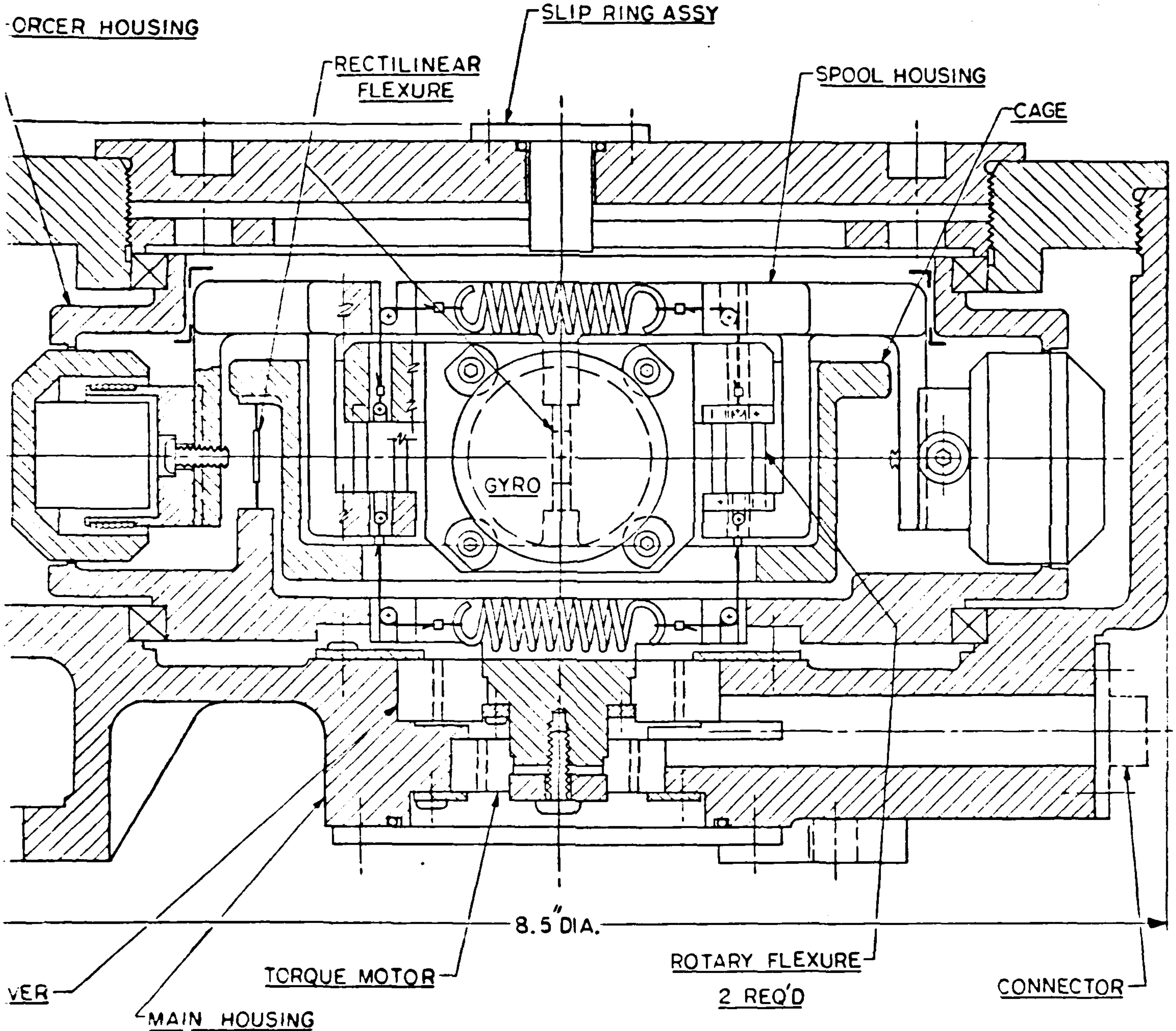

Fig. (A)

MAY 24 1984

REV	DESCRIPTION	DWN	CKD	DATE

NOTES
1 DO NOT SCALE THIS DRAWING
2 BREAK ALL SHARP CORNERS
3 TOLERANCES EXCEPT AS NOTED
DECIMALS ± .005
FRACTIONS ± 1/64
ANGLES ± 1°

MICRO INCHES	DESCRIPTION
4	PRECISION POLISH
8	FINE POLISH
16	COMMON POLISH
32	GRIND OR EQUAL
63	SMOOTH MACH
125	COMMON MACH
250	ROUGH MACH
500	HEAVY MACH
1000	EX HEAVY MACH

GYROART — OAKLEAF AVENUE · AGOURA, CALIF.

GYRO ASSEMBLY

DWN	DATE 5/19/84	SCALE 2/1	1007
CKD	DATE		

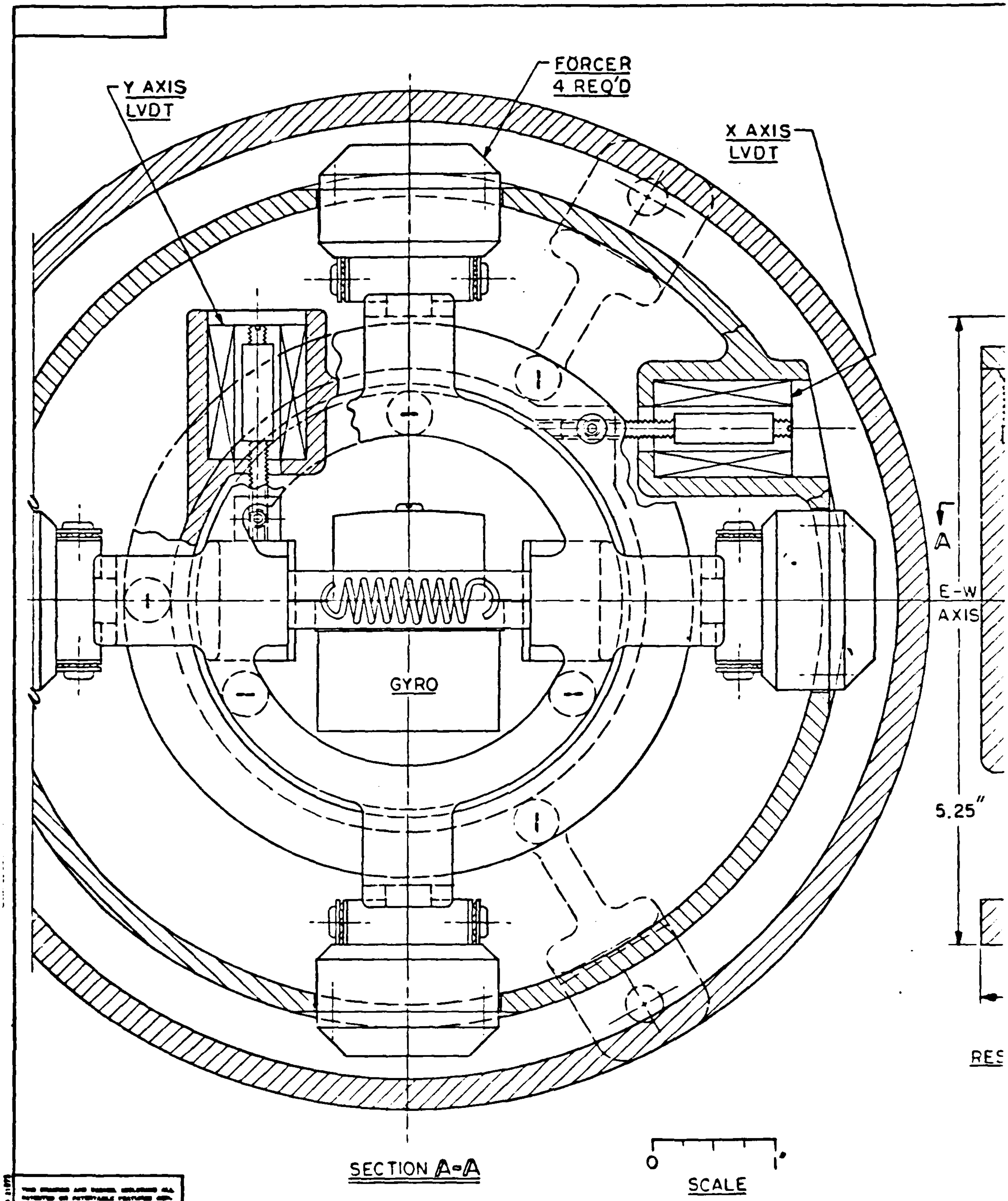
FORCER
4 REQ'D
Y AXIS
LVDT
X AXIS
LVDT
GYRO
A
E-W
AXIS
5.25"
RES
SECTION A-A
0
1"
SCALE

Fig. (

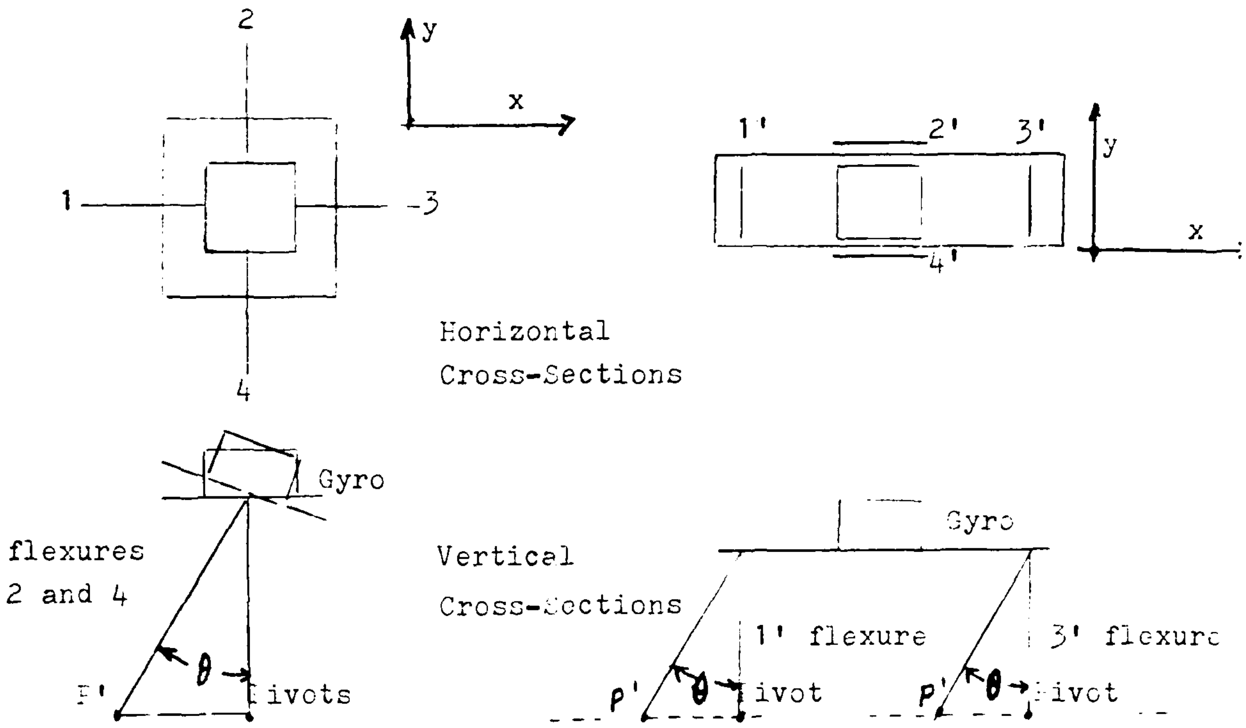

fig. (B)

Pendulous Suspension
(former design)

fig. (C)

Rectilinear-Parallelogram Suspension
(current design)

In fig. (A), motion of the pivots to the left (-x) to P' causes the gyro to rotate through θ with disasterously large angular rates. (Flexures 2 and 4 absorb motion in the x direction.)

In fig. (B), motion of the pivots to the left (-x) to P' causes the gyro to merely translate but without rotation. The gyro platform remains parallel to the base. (Flexures 1' and 3' absorb motion in the x direction.)

Thus, the simple act of rotating the flexures 90° with respect to the base has eliminated the induced rotations of the pendulum.

While the contract specifications for the gyrocompass only refer to tilt rates of 1.5 milliradians per minute, we must assume that there are also angular vibration inputs present in a real vehicle scenario. To accomodate this disturbance, the gyro is mounted to the rectilinear flexure by low friction bearings through the center of gravity along the east-input axis. (Angular vibrations about the gyro spin axis are not important to system performance so provisions are not made for these disturbances.) The low-friction bearings are made of cross-spring flexures, thus the natural frequency of the gyro about the suspension axis is very low compared to the frequency of the angular vibration inputs. Thus, the gyro remains nearly fixed in inertial space as the frame rotates around it. Steady "D.C." earth rate terms are transmitted to the east-axis of the gyro via a the cross-spring gyro suspension bearings.

The rectilinear suspension was examined to determine the effect of dimensional tolerances on suspension effectiveness. The length of one arm was varied in steps of .001" and the change in platform level of the gyro platform was then computed for a 1° rotation of the arms. The level (tilt) did not change more than 10^{-7} radians over the 1° rotation. The following figure illustrates this result.

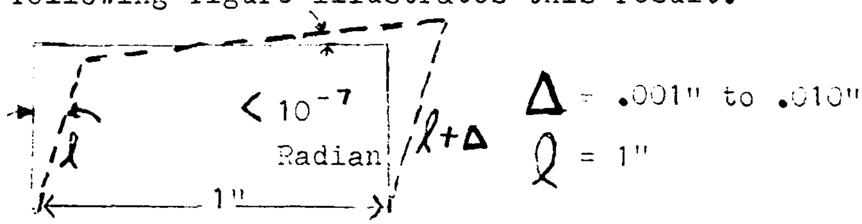

The rotational de-coupling of the gyro provided by the low friction, low natural frequency bearing was also analyzed. For a 10 to 1 ratio of excitation frequency to suspension-natural frequency, the gyro remained stationary with respect to space with only a .4% error. (99.6% of the frame vibrations were filtered out.)

III. Isolation System Design Description and Analysis

The siesmic isolation concept uses proven techniques which have been applied in a wide variety of engineering problems. These range from wind tunnel model mounting systems to gravimetric devices.

The result of placing the rate gyro on such a suspension is to detach it from all periodic disturbances both linear and angular. Only a "D.C." rate is transmitted through the mounting means unimpeded.

The physical implementation involves the use of a linear isolation system to a fixed structure which filters out all linear vibrations. Mounted on the linear isolator is a rotary isolator. The function of the rotary isolation system is to provide a friction-free suspension about the east-west axis of the rate gyro. Because this axis is completely unconstrained, angular vibrations about it cannot affect the gyro.

The actual mechanization of these ultra-low pass mechanical filters is simple and straightforward. The relationship between the amplitude X of the imposed periodic motion and the relative displacement of the suspended mass Z is given by the expression,

$$Z = \frac{X}{\left(\frac{Wn}{W}\right)^2 - 1} \qquad \text{(No Damping)}$$

As the natural frequency Wn of the suspension approaches zero, the relative motion of the suspended mass becomes equal and opposite to the imposed motion X. The mass remains decoupled from the imposed motion and therefore the gyro which is attached to it is not affected by disturbances applied to the support structure.

The use of the "stepped leg" construction permits the use of very limber flexures while avoiding the possibility of their failure in the buckling mode. The dimensions chosen in the actual embodiment result in a ratio of the applied load to the calculated buckling load of 45%. The applied load is that spring force required to make the suspension astatic, that is, infinitly compliant. Because the flexures are comparatively short, the Euler loads (buckling force) becomes relatively large.

Thermal effects are reduced to nil by virtue of the fact that the materials used in the construction of the flexures and the loading spring display a constant elastic modulus over a wide temperature range.

To isolate periodic base motions in both side to side and front to back directions the siesmic suspension is arranged in a nested fashion. The suspension which isolates the gyro from side to side motion carries a second, orthogonal, suspension assembly which eliminates the effects of front to back base disturbances.

The linear variable differential transformers which detect orthogonal components of base motion are arranged to eliminate the effects of interaxis cross coupling.

In addition to the system just described which effectively eliminates the effect of translatory disturbances on the gyro. A rotary suspension supports the gyro on its east-west axis to filter out rational vibrations. In the cross spring pivot which serves as the east-west bearing for the gyro, a spring is used to load the flexures in tension. The relation of the bending moment about the center and the axial force is shown in the figure below.*

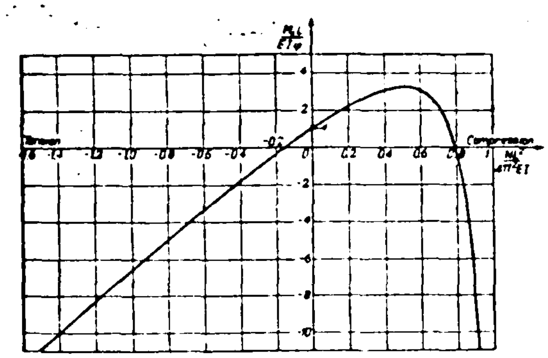

The ordinate is the quantity, $\frac{M}{\theta} \cdot \frac{L}{EI}$

$\frac{M}{\theta}$ is the torque per unit of angular rotation. L is the flexure length. EI is the product of the moment of inertia of the blades and the modulus of elasticity of the blade material. The abcissa is $\frac{NL^2}{4\pi^2 EI}$ where N is the normal load on the flexure pivot. The significant point on the curve is its intercept on the negative abcissa. At this point resistance to pivot rotation becomes zero. For a value of the abcissa equal to one, the crossed pivot carries a compressive load equal to the Euler or buckling load.

From the figure it can be seen that a properly designed and loaded pivot will exhibit astatic behavior under a tensile preload which is less than twenty percent of the compressive buckling load.

The suspension loading spring applies a force which is about twenty times as great as the weight of the gyro and associated mounting plate so that shock loading and other extraneous forces

*(Taken from "Note on Frictionless Bearing for Small Angular Deflections" by J.A. Haring - Journal of Applied Physics, Dec. '4 .

have a diminishingly small effect on the structure. The ruggedness and simplicity of the construction recommends it.

In summary, environmental vibration can be effectively filtered through the use of a low-cost mechanical suspension system which exhibits the astatic property (zero friction and infinite compliance). There are no "grey" or questionable areas in the design since all of the concepts, materials and fabrication techniques involved are proven and within the state-of-the-art.

APPENDIX B

Preliminary Servo Designs

1. Capture Loop Analysis/Design

The pendulum capture loop has been refined to improve its performance in the presence of static and dynamic disturbance. The table below shows the steady state performance of the design in response to specified expected disturbances.

Disturbance	Hang-off Angle	Hang-off Angle Rate
Constant Tilt	None	None
1.2 mr/min tilt rate	2.6 * 10 [illegible] rad	None
$14.7 * 10^{-3}$ g @ 6 cps	$1.28 * 10^{-9}$ rad @ 6 cps	.01 deg/hr @ 6 cps

The block diagram below illustrates the current configuration.

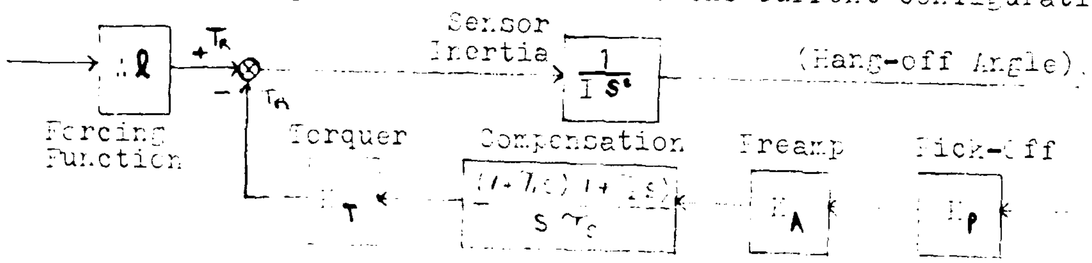

Where K_p = 27.8/8 volt/rad
K_T = 3.75/1.2 in-lb/volt
K_A = 35 v/v
τ_1 = 2 sec.
τ_s = .0025 sec.
I = $1.035 * 10^{-2}$ in-lb-sec^2
$W\ell$ = 2 in-lb.

with the frequency variable function KG(s) being implemented as follows

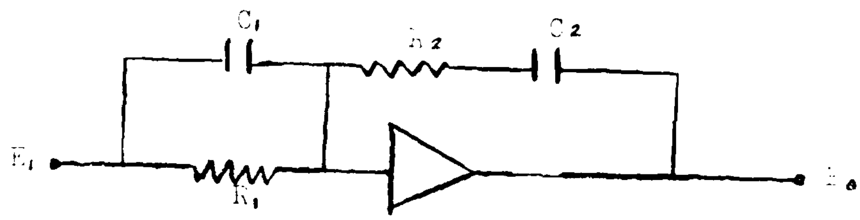

$$\frac{E_o}{E_i} = \frac{(1+SR_1C_1)(1+SR_2C_2)}{SR_1C_1}$$

The advantages the current design offers over the initial design include

a.) Elimination of steady state hang-off due to fixed case tilt angle.

b.) Elimination of constant rate of growth hang-off angle in the presence of constant case tilt rate.

c.) Orders of magnitude reduction of induced angular rates in the presence of horizontal linear case vibrations.

II. Azimuth Servo Analysis

As initial design of the azimuth servo has been generated from the standpoint of isolating the sensing gyro from azimuth angular disturbances. For this initial design effort, the goal was to achieve a reduction of an angular disturbance of the azimuth muth gimbal by a factor of 100 in .1 seconds. The mechanization considered uses the gyro azimuth axis to sense the disturbance and provide an error signal to drive the gimbal torquer via the stabilization and driver electronics. The following block diagram depicts this configuration.

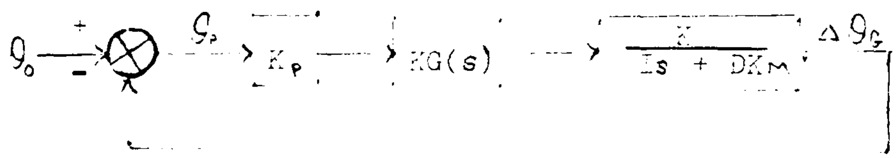

θ_p = Pick-Off Angle

$\Delta\theta_3$ = Gimball Angle Change

$\Delta\theta_3(s)$

K_p = 675 volt/rod

K_m = .3243 oz-in/volt

D = .042 volt/(rod/sec)

I = .03 oz-in-sec^2

The transfer function relating pick-off angle to an input azimuth gimbal angle disturbance is

$$\frac{\theta_p}{\theta_0} = \frac{s\,(s + DK_m/I)}{s^2 + DK_m/I\,s + K_p K_m KG(s)/I}$$

Without compensation the basic system is highly oscillatory and lightly damped. To provide a rapid and well damped reduction of the input disturbance the following stabilization function was arrived at

$$KG(s) = 1 + \tau s \,,$$

With this compensation, the time solution for a step input is

$$\frac{\theta_p}{\theta_0}(t) = 1.395 \, e^{-59.75t} \sin(3495t + 134.2^\circ)$$

and at the end of .1 sec., an initial angular error is reduced by a factor of .003. Subsequent design analyses will investigate the effects of time varying disturbances.

APPENDIX C

Gyro Drift Stability Test Data

Analysis of Conex Gyro

The following graphs show the short term stability of the Conex gyro about both measuring axes. Here, the RMS drift rate change between successive samples of duration "t" are shown. Thus, successive 2 minute samples will have an RMS drift rate stability (change) not exceeding .002 deg/hr.

This is the method that the Gyroart gyro output will be sampled to simultaneously determine north and the gyro bias (two step gyrocompassing). This corresponds to .2 mils heading error (RMS).

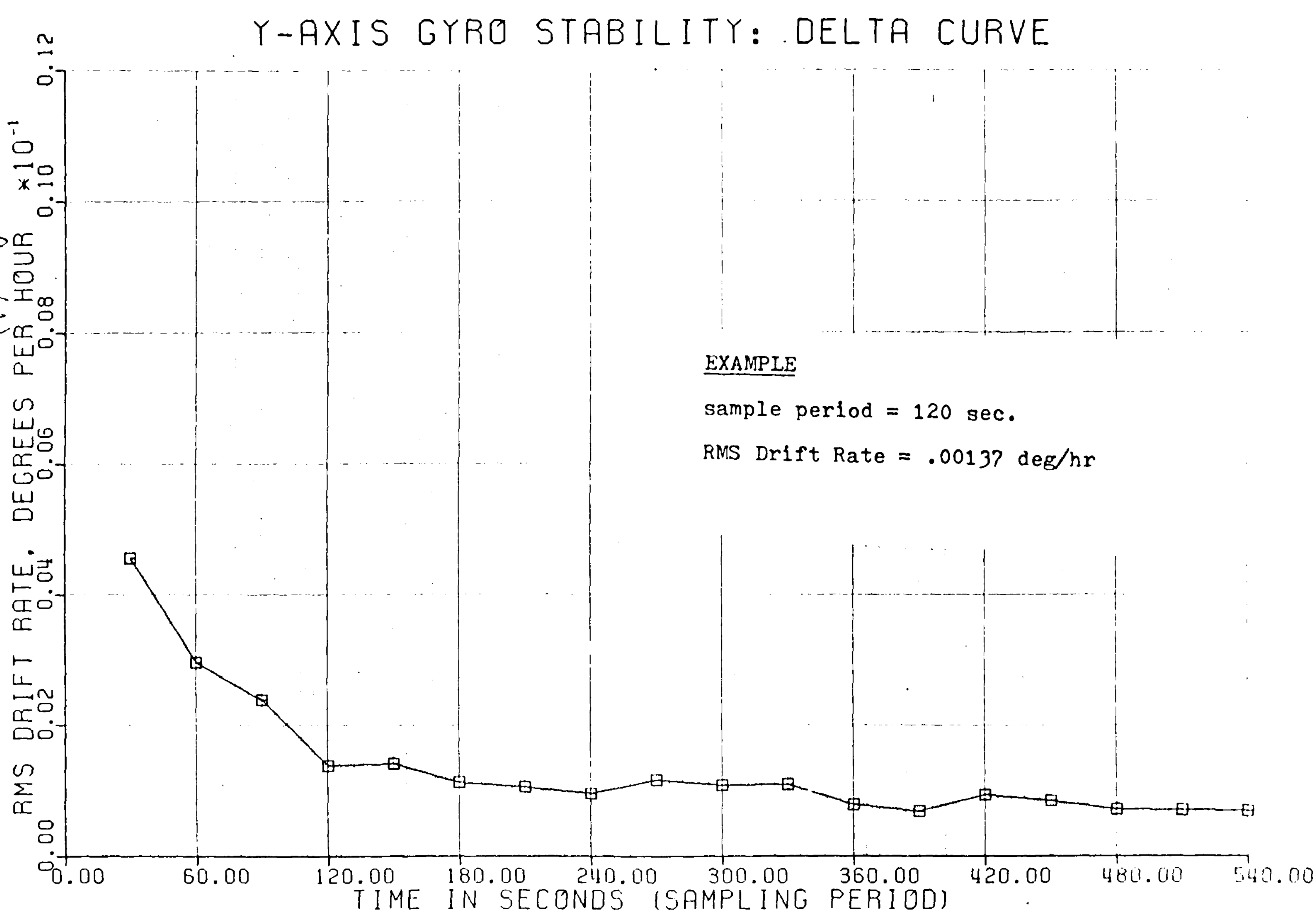
Y-AXIS GYRO STABILITY: DELTA CURVE
RMS DRIFT RATE, DEGREES PER HOUR ×10⁻¹
0.00
0.02
0.04
0.06
0.08
0.10
0.12
0.00
60.00
120.00
180.00
240.00
300.00
360.00
420.00
480.00
540.00
TIME IN SECONDS (SAMPLING PERIOD)
EXAMPLE
sample period = 120 sec.
RMS Drift Rate = .00137 deg/hr

C-3

fig (A)

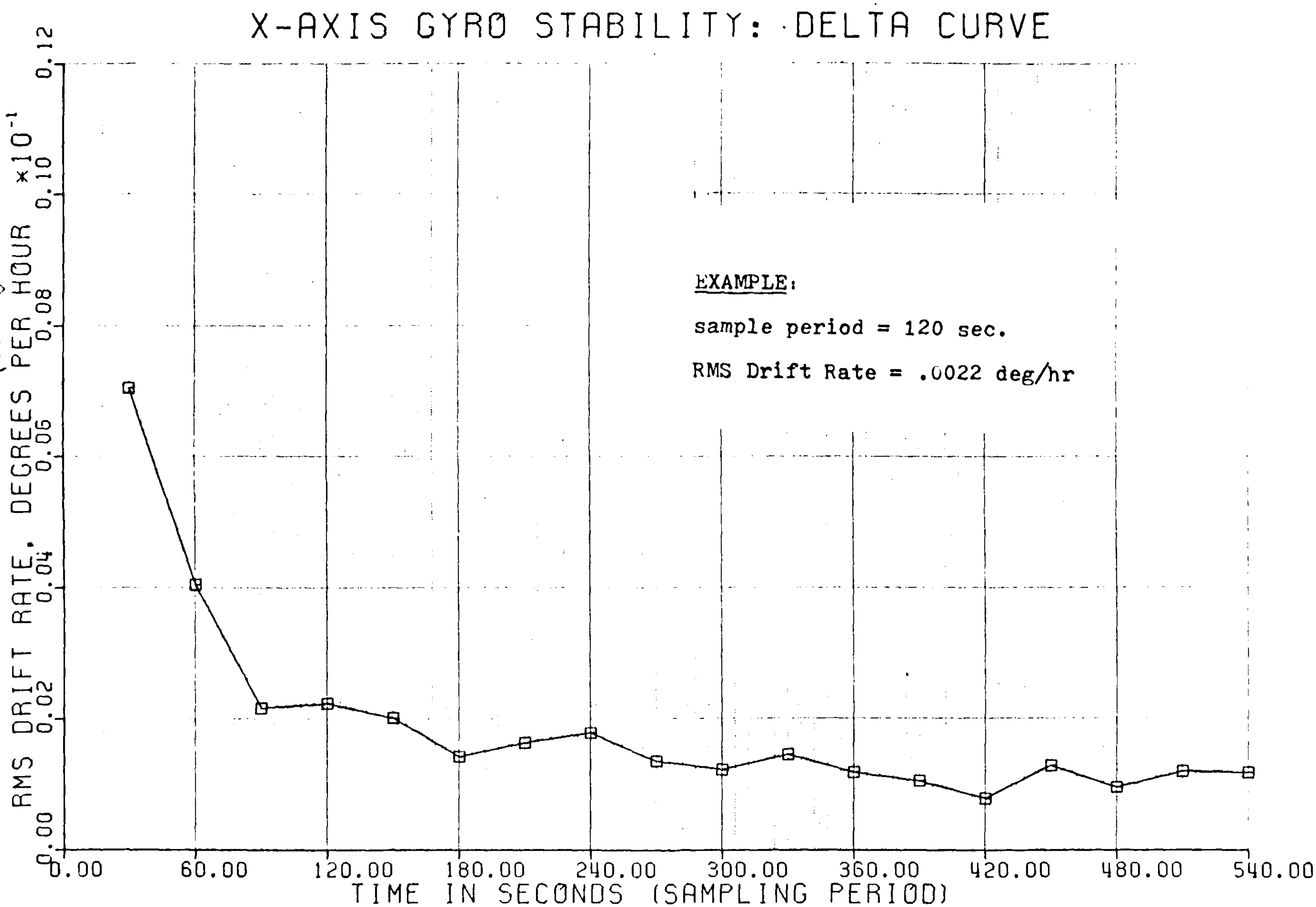

X-AXIS GYRO STABILITY: DELTA CURVE
RMS DRIFT RATE, DEGREES PER HOUR ×10⁻¹
0.00
0.02
0.04
0.06
0.08
0.10
0.12
0.00
60.00
120.00
180.00
240.00
300.00
360.00
420.00
480.00
540.00
TIME IN SECONDS (SAMPLING PERIOD)
EXAMPLE:
sample period = 120 sec.
RMS Drift Rate = .0022 deg/hr

C-4

APPENDIX D

Kalman Filter Design

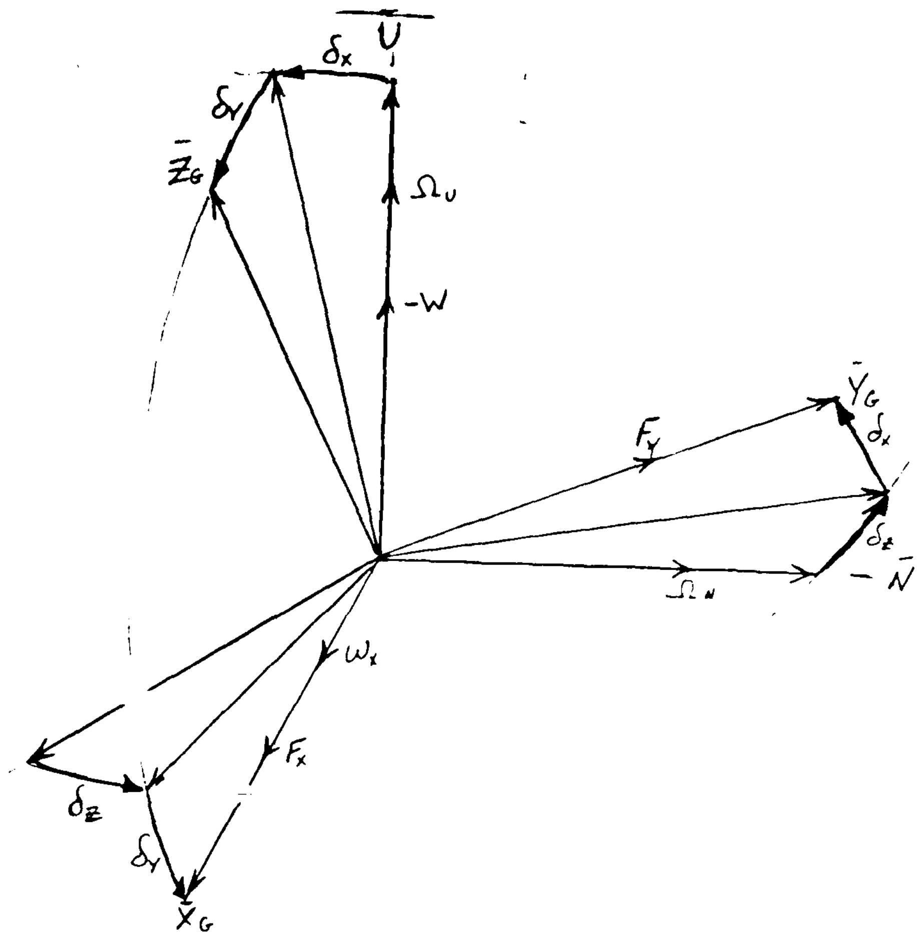

Let $\bar{X}_G, \bar{Y}_G, \bar{Z}_G$ be gyro coordinates misoriented with respect to local coordinates $\bar{E}_{ast}$, $\bar{N}_{orth}$, $\bar{U}_p$ by angles $\delta_z, \delta_y, \delta_x$. The coordinate sets are related as follows

$$\begin{vmatrix} X_G \\ Y_G \\ Z_G \end{vmatrix} = \begin{bmatrix} (c\delta_z c\delta_Y - s\delta_z s\delta_x s\delta_Y) & (s\delta_z c\delta_Y + c\delta_z s\delta_x s\delta_Y) & -c\delta_x s\delta_Y \\ -s\delta_z c\delta_x & c\delta_z c\delta_x & s\delta_x \\ (c\delta_z s\delta_Y + s\delta_z s\delta_x c\delta_Y) & (s\delta_z s\delta_Y - c\delta_z s\delta_x c\delta_Y) & c\delta_x c\delta_Y \end{bmatrix} \begin{vmatrix} E \\ N \\ U \end{vmatrix}$$

For sufficiently small angles, this expression reduces to

$$\begin{vmatrix} X_G \\ Y_G \\ Z_G \end{vmatrix} = \begin{bmatrix} 1 & \delta_z & -\delta_Y \\ -\delta_z & 1 & \delta_x \\ \delta_Y & -\delta_x & 1 \end{bmatrix} \begin{bmatrix} E \\ N \\ U \end{bmatrix}$$

This resulting small angle transformation describes three independent angular rotations, each being taken about one of the local coordinates. The total misalignment vector can then be described by; $\bar{\Phi} = \phi_E \bar{E} + \phi_N \bar{N} + \phi_U \bar{U}$ where ϕ_E and ϕ_N are the tilt angles about $\bar{E}$ and $\bar{N}$ respectively and is the true azimuth misalignment about $\bar{U}$.

Considering a non-vibration case where the pendulum is tightly captured to the case, the force and rate measurements in gyro/care coordinates can be written as;

$$\begin{bmatrix} F_X \\ F_Y \end{bmatrix} = \begin{bmatrix} 1 & \phi_U & -\phi_N \\ -\phi_U & 1 & \phi_E \end{bmatrix} \begin{bmatrix} 0 \\ 0 \\ W \end{bmatrix} \qquad (\text{since } \bar{F} = -\bar{W})$$

$$\begin{bmatrix} \omega_x \end{bmatrix} = \begin{bmatrix} 1 & \phi_U & -\phi_N \end{bmatrix} \begin{bmatrix} 0 \\ \Omega_N \\ \Omega_U \end{bmatrix} + \begin{bmatrix} 1 & 0 & 0 \end{bmatrix} \begin{bmatrix} \dot{\phi}_E \\ \dot{\phi}_N \\ 0 \end{bmatrix}$$

These can be combined in terms of a single measurement vector;

$$\begin{bmatrix} F_X \\ F_Y \\ \omega_x \end{bmatrix} = \begin{bmatrix} 0 & -W & 0 & 0 & 0 \\ W & 0 & 0 & 0 & 0 \\ 0 & -\Omega_U & \Omega_N & 1 & 0 \end{bmatrix} \begin{bmatrix} \phi_E \\ \phi_N \\ \phi_U \\ \dot{\phi}_E \\ \dot{\phi}_N \end{bmatrix}$$

This can also be written as

$$\bar{Z} = H\bar{X}$$

where, $\bar{Z}$ = Measurement vector $[F_x \quad F_y \quad W_x]^T$

$\bar{X}$ = State Vector $[\phi_E \quad \phi_N \quad \phi_U \quad \dot{\phi}_E \quad \phi_N]^T$

H = Observation Matrix $\begin{bmatrix} 0 & -W & 0 & 0 & 0 \\ W & 0 & 0 & 0 & 0 \\ 0 & -\Omega_U & \Omega_N & 1 & 0 \end{bmatrix}$

Assuming tilt rates $\dot{\phi}_E$ and $\dot{\phi}_N$ are constant over the sample interval Δt, the change in the state vector over the interval can be expressed as;

$$\begin{bmatrix} \phi_E \\ \phi_N \\ \phi_V \\ \dot{\phi}_E \\ \dot{\phi}_N \end{bmatrix}_m = \begin{bmatrix} 1 & 0 & 0 & \Delta t & 0 \\ 0 & 1 & 0 & 0 & \Delta t \\ 0 & 0 & 1 & 0 & 0 \\ 0 & 0 & 0 & 1 & 0 \\ 0 & 0 & 0 & 0 & 1 \end{bmatrix} \begin{bmatrix} \phi_E \\ \phi_N \\ \phi_V \\ \dot{\phi}_E \\ \dot{\phi}_N \end{bmatrix}_{m-1}$$

or in shorthand notation; $\bar{X}_n = \underline{\Phi}\bar{X}_{n-1}$, where $\underline{\Phi}$ is the state transition matrix.

To complete the Kalman filter formulation, some other quantities should be defined. e.g.

1. The measurement error covariance matrix, R associated with the errors in the force and rate measurements. Assuming the errors are gaussian and uncorrelated, R is a diagonal matrix consisting of the variances in the force and rate measurements

$$R = \begin{bmatrix} \sigma_{Fx}^2 & 0 & 0 \\ 0 & \sigma_{Fy}^2 & 0 \\ 0 & 0 & \sigma_{\omega}^2 \end{bmatrix}$$

2. The error covariance in the estimation of the states, P. P is a square symmetrical matrix whose dimensions are equal the number of states, in this case 5*5.

3. The covariance describing the "plant" or "process" noise, Q. Q has the same dimensions as P. In this case, Q would represent the noise due to vibration (if one knew how to model it).

To simulate the Kalman filter, use the following approach

1. Filter Initialization:

   a.) Set the state vector $\bar{X}$ equal to zero.
   b.) Set the diagonal elements of P to some reasonable values.
   c.) Set Q equal to zero.
   d.) Define R covariance, Φ matrix and H matrix
   e.) Set K equal to zero (5*5 matrix).

2. Problem Initialization

a.) Set t equal to zero.

b.) Set value of Δt.

c.) Set true values of initial misalignment angles and tilt rates $\gamma_{E_0}, \gamma_{N_0}, \gamma_{U_0}, \dot{\gamma}_E, \dot{\gamma}_N$.

d.) Set latitude.

e.) Determine Ω_N, Ω_U; $\Omega_N = \Omega_E \cos(LAT)$; $\Omega_U = \Omega_E \sin(LAT)$.

f.) Set value of W.

g.) Set values of C_x, C_y, C_w and $\sigma_{F_X}, \sigma_{F_Y}, \sigma_W$ (same as in R).

3. Problem Solution

$$t = t + \Delta t$$

$$\gamma_E = \gamma_{E_0} + \dot{\gamma}_E t$$

$$\gamma_N = \gamma_{N_0} + \dot{\gamma}_N t$$

$$F_x = -W\gamma_N + C_x \sigma_{F_x}$$

$$F_Y = W\gamma_E + C_Y \sigma_{F_Y}$$

$$\omega_x = \Omega_N \gamma_{U_0} - \Omega_U \gamma_{N_0} + \dot{\gamma}_E + C_\omega \sigma_\omega$$

$$\bar{Z}_n = (F_x, F_Y, \omega_x)^T$$

$$P_n^- = \Phi P_{n-1} \Phi^T + Q$$

$$K_n = P_n^- H^T (H P_n^- H^T + R)^{-1}$$

$$P_n^+ = (I - K_n H) P_n^-$$

Print values of t, P_n^+, $\bar{X}_n$, differences between $\bar{X}_n$ and γ_E, $\gamma_N, \gamma_U, \dot{\gamma}_E, \dot{\gamma}_N$.

Return to start of 3 and interate.

<u>Note:</u> From a programming standpoit there is no need to specify seperate variable names for P_n^-, P_{n-1} and P_n^+. A single variable name would do. The same is true for $\bar{X}_n$ and $\bar{X}_{n-1}$. Doing this, steps $P_{n-1} = P_n^+$ and $\bar{X}_{n-1} = \bar{X}_n$ are not required.

The estimated states ϕ_E, ϕ_N, ϕ_V only define the orientation of the gyro/azimuth gimbal coordinates. The true azimuth of the case (ψ_c) can be found from;

$$\tan \psi_c = \frac{s\rho + \phi_v c\rho}{c\rho - \phi_v s\rho}$$

where ρ is the azimuth gimbal angle whose positive direction is defined by;

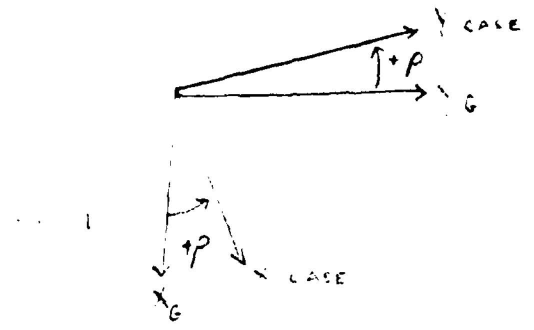

APPENDIX E

Experimental Evaluation of the Static Efficiency
of the Gyroart Rectilinear-Flexure Suspension

I. Summary of Results and Conclusions

A model of the special Gyroart double tripod rectilinear flexure support was fabricated to test the ability of the support to minimize the effect of rotation at the gyroscope mounting surface associated with relative translational motion of the base of the support with respect to the mounting surface.

The experimental evidence presented in this report clearly shows that a very large decrease in mounting surface rotation due to relative base translation is achieved by utilizing a parallelogram tripod knife-edge arrangement of flexure suspension in contrast to a single pendulum-type suspension, which provides no isolation from this effect.

Using the experimental model, it was determined that, even in the extreme case with an equivalent pendulum rotation of about 2.3 degrees (full travel of inner suspension ring) the mounting surface tilted about 1/120 of this or .019 degrees. It is also noted that the flexure support "fully loaded down" i.e. near buckling, provided a very large amount of isolation from base motions as expected, although further dynamic tests will be required to quantify this observation.

II. Test Procedure

The tilt tests were performed using a flexure support fabricated by Galiso, Inc., Anahiem, California, especially for the tests. A Kearfott B1802 Electrolytic-type tilt angle sensor was calibrated at the test site as explained below, and mounted on the inner ring of the flexure support. The inner ring was then moved from side to side until it contacted the outer ring. Readings from the tilt sensor were taken at reference (center) position and then at the two extreme positions on either side of center. Using the calibration data, the measurements were translated into total tilt about the axis of rotation.

The calibration of the tilt angle sensor was carried out as follows:

The tilt angle sensor was fastened to the base of the flexure support platform. The platform was placed on a granite flat table (see photos) with a sine bar between the platform and the flat table. One end of the sine bar rested on the flat table, the other was suspended by a vertial micrometer arrangement (see photos). The tilt angle sensor was excited with a 20 VAC @ 400 HZ source and the output was measured with a 5½ digit DMM.

Measurements of tilt taken as AC volts were taken from the tilt angle sensor as the vertical micrometer was moved up increasing the tilt of the base. The micrometer readings were then converted to angles of tilt (see calculations). From the calibration data, a calibration curve was plotted and a rough linear estimate of the output/tilt angle was made. This information was used to interpret the actual tilt test results.

III. Flexure Support Model

A model of the proposed Gyroart double tripod knife-edge flexure support was built to about twice the final design size to exhibit the tilt isolation and base motion isolation features of the overall design. The flexure joints were fabricated using 1.5 inch lengths of tempered steel clock spring wire .01 inch by .125 inch cross-section, sharpened at one end. The flexures were mounted in an ingenious double tripod parallelogram configuration (see photos and explanation in other sections of this document). The retaining rings and support structure were fabricated from aluminum. Notches were made in the retaining rings so that the free ends of flexures could act as knife edges.

The flexure suspension mechanism thus constructed was then placed on an outer support structure and loaded in compression with a spring tension member through the center of the inner support ring (see photos).

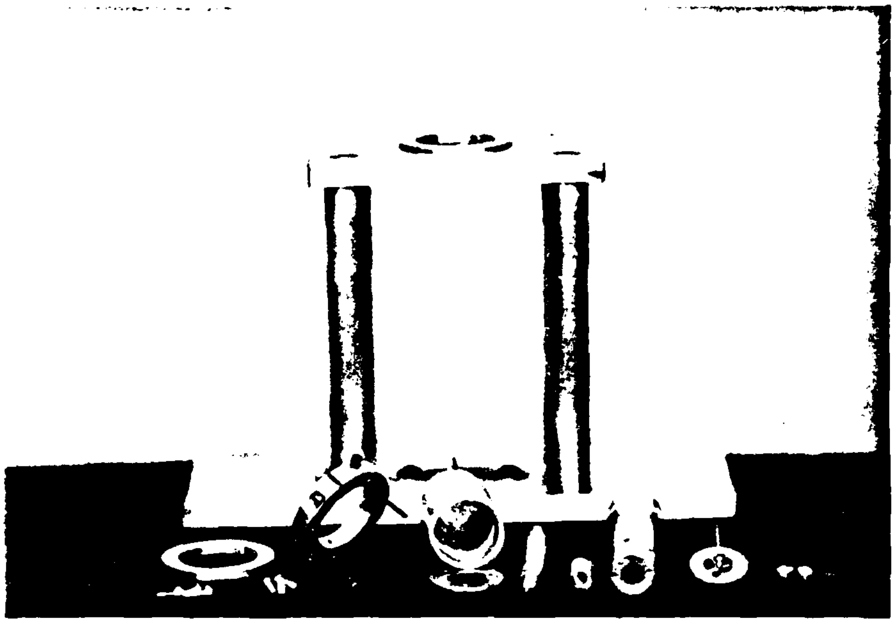

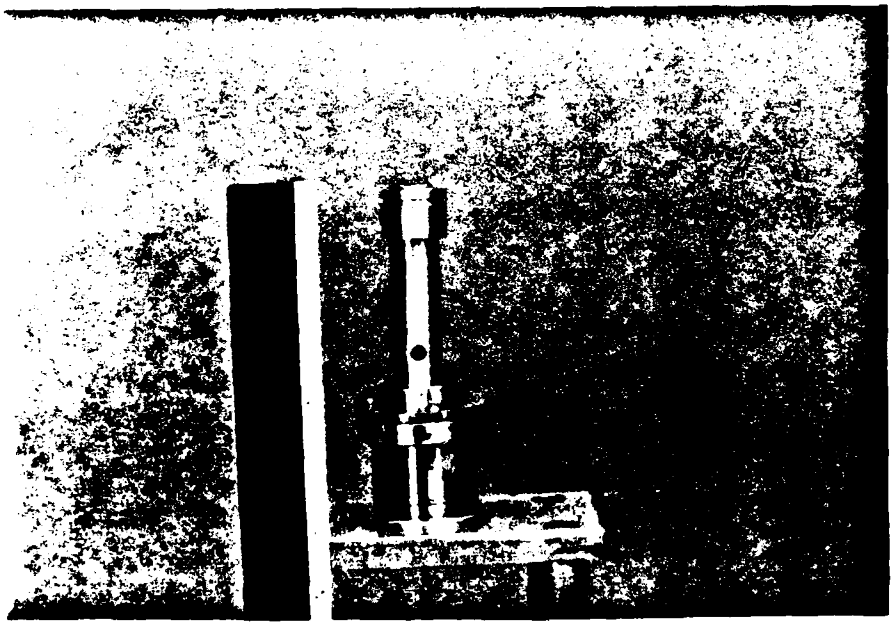

Fig.(4)

GYROART RECTILINEAR FLECTURE TEST MODEL

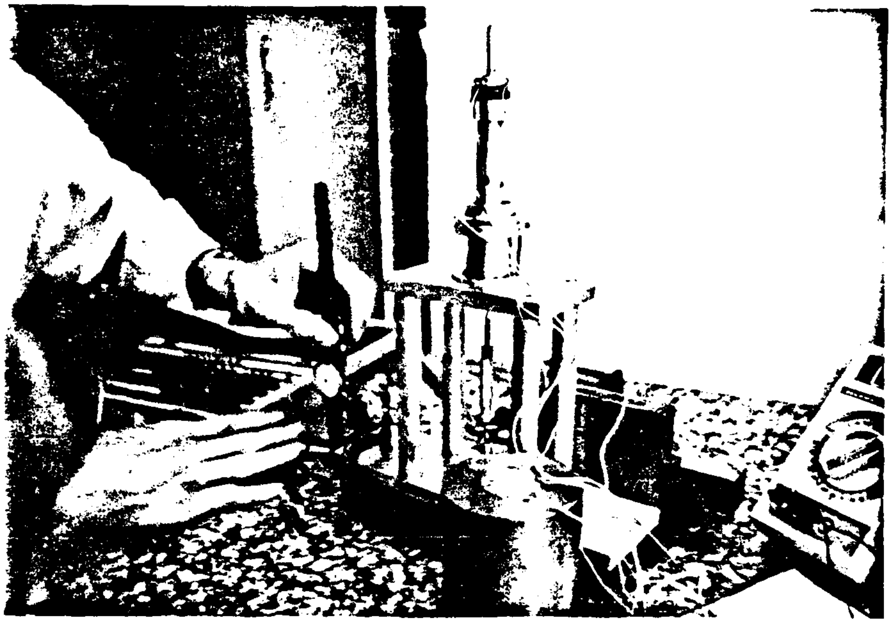

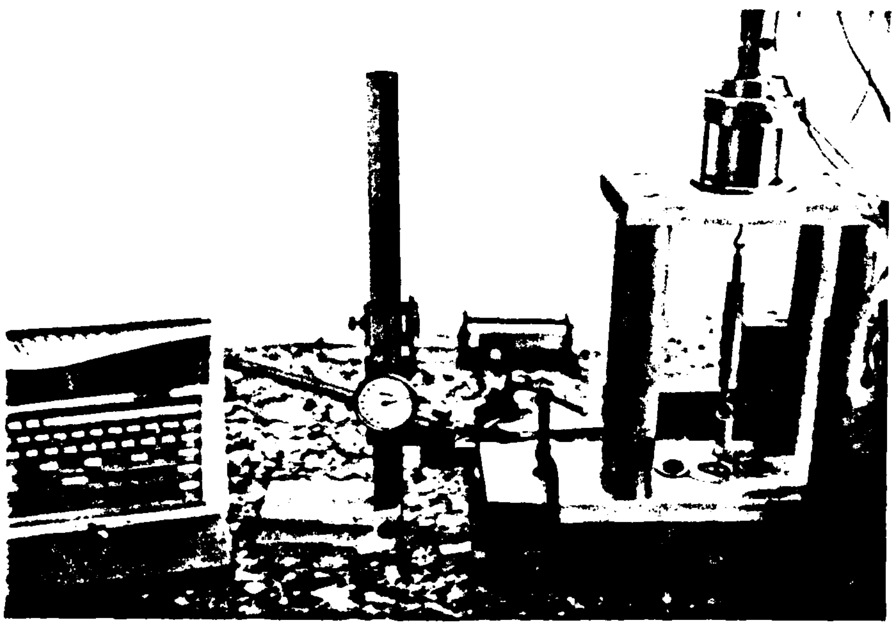

Fig. (3) FLECTURE SUPPORT TEST SETUP

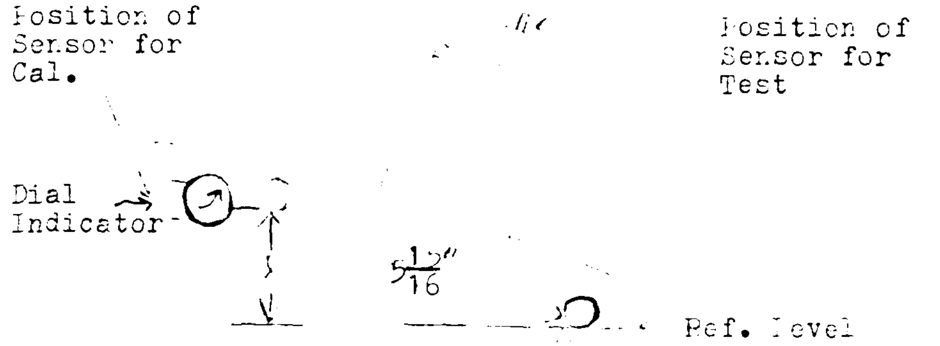

Vin = 26 VAC RMS
@ 400 Hz.

Fig. (c)

Equipment: Dana model 5000 DVM CAL 22/3/84
Calif. Inst. AC power source
model 251T. Kearfott 1802
Vertical Sensing Inst.
Beckman Tech. 300 DVM (Ref. only).

Sensor Calibration Data

Dial In. $\times 10^3$	E_{2-4} VAC RMS	E_{1-3} VAC RMS	α [illegible]
60	1.405	.3001	0
65	1.412		.0462
70	1.425		.0965
75	1.428		.1447
80	1.435		.1930
85	1.439		.2412
90	1.446	.3004	.2895
95	1.465		.3377

Test measurements

1.) Sensor vertical = 1.027, E_{1-3} = .2010
2.) Push to right → E_{2-4} = 1.026 V
3.) Push to left ← E_{2-4} = 1.029

Fig. (7)

For small angles (2 or less) take sin for sine block measurements. = 5.9375α ,

Total Angle of Rotation of Equivalent Simple Pendulum

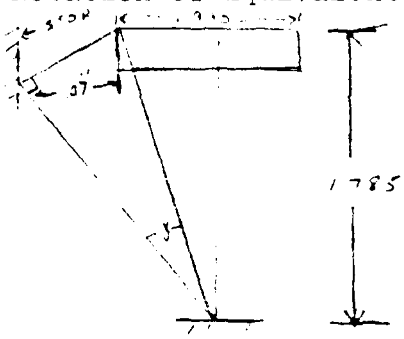

$\gamma \approx \sin^{-1} \frac{.07}{1.785}$

data from experiment yields:

ΔE_{max} = .002 VAC RMS

= .0192°

So, E/θ = 2.29 / .0192

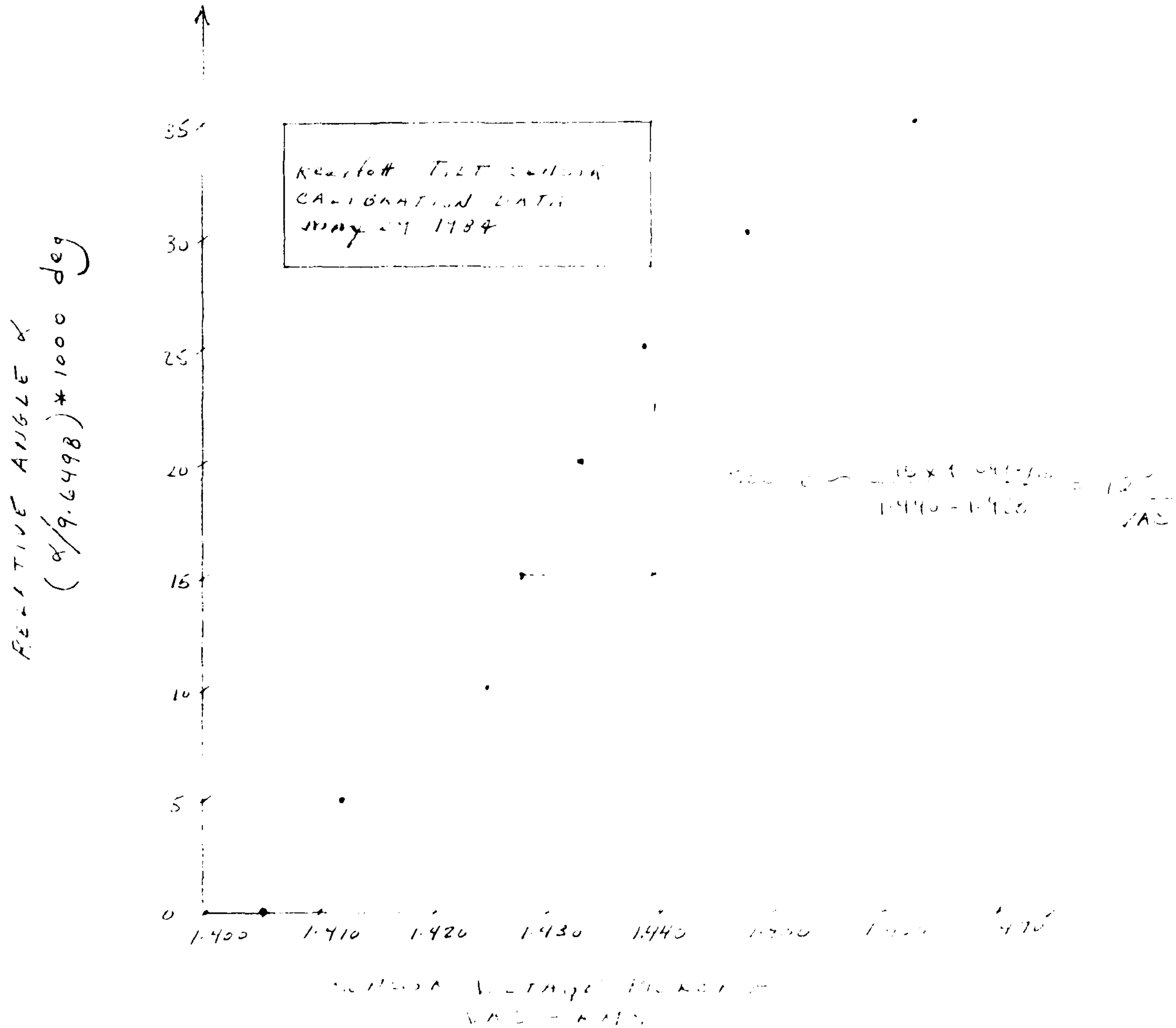
RELATIVE ANGLE α
(α/9.6498)*1000 deg
0
5
10
15
20
25
30
35
1.400
1.410
1.420
1.430
1.440
CALIBRATION DATA

Fig. (E)

END

DATE
FILMED

1-85

DTIC